Optimization of Low-Loss Al_2O_3 Waveguide Fabrication for Application in Active Integrated Optical Devices

K. Wörhoff, F. Ay, and M. Pollnau

Integrated Optical MicroSystems Group
MESA+ Research Institute, University of Twente
P.O. Box 217, 7500 AE Enschede, The Netherlands, e-mail: k.worhoff@ewi.utwente.nl

In this paper we will present the fabrication and properties of reactively co-sputtered Al_2O_3 layers, being a very promising host material for active integrated optics applications such as rare-earth ion doped laser devices. The process optimization towards a reactive co-sputtering process, which resulted in stable, target condition-independent deposition of Al_2O_3 layers with high optical quality will be discussed in detail. The loss value of as-deposited optical waveguides sputtered by the optimized process has been measured. The loss in the near infrared wavelength range was 0.3 dB/cm. Furthermore, Al_2O_3 material hosts fabricated by sputtering techniques are compatible with Si-based integrated optical technology and allow for uniform deposition over a large substrate area.

Introduction

Amorphous aluminum oxide (Al_2O_3) is a very promising host material for active integrated optics applications such as rare-earth-ion doped laser devices. Over the past decade various research groups have developed Al_2O_3 deposition processes based on different techniques: pulsed laser deposition (PLD) (1), (2), atomic layer deposition (ALD) (3), (4), chemical vapor deposition (CVD) (5), (6), sol-gel method (7), (8), (9) sputtering from a dielectric target (10), (11) and reactive co-sputtering based on a metallic target (12), (13).

In general, thin films for integrated optical (IO) waveguides should fulfill the following requirements: low propagation loss, reproducible layer thickness and refractive index over a large substrate area and sufficiently high deposition rate in order to enable waveguide fabrication up to the micron thickness range. Moreover, for devices based on rare-earth ion transitions OH-free deposition is required, because these bonds form one of the major quenching sources and will largely diminish the gain efficiency. When comparing the typical properties of previously applied deposition techniques, it becomes obvious that CVD and sol-gel techniques suffer from OH incorporation, due to the presence of hydroxyl groups in the process precursors. The application of ALD for optical waveguides, although resulting in thin films with excellent quality, is rather limited due to the extremely low deposition rate, which typically results in film thicknesses up to several tens of nanometers. The main draw-back of the PLD technique consists in the limited substrate area (typically 1-3 cm range) which can be covered by a thin film with acceptable uniformity. This size limitation will restrict the integration scale

of complex IO devices. Based on the results of previous studies, the sputtering technique can be considered to be very promising for the fabrication of amorphous Al_2O_3 for integrated optics since it combines an inherently low OH-content with relatively fast, uniform and controlled deposition over a large substrate area.

Although rare-earth doped Al_2O_3 waveguides have already been demonstrated to be an attractive material system for integrated optical amplifiers and tunable light sources (14), (13), the previous studies still yield some disadvantages which had to be overcome. The propagation loss values for Al_2O_3 slab waveguides reported in (14) was optimized to 0.35 dB/cm, however only after an additional annealing step which reduced the loss of the as-deposited layers being as high as 20 dB/cm. Moreover, the active ions had to be introduced by ion implantation and annealing steps, what leads to an increase in processing complexity. To the best reported background loss of Er: Al_2O_3 waveguides belongs an estimated value of about 0.25 dB/cm (13) obtained by reactive co-sputtering based on DC-driven sputtering guns. The main drawback of the applied method turned out to be the poor process stability and reproducibility, which was highly dependent on the exact condition of the sputtering target.

In this paper a comparative study between DC and rf-based reactive co-sputtering of Al_2O_3 waveguides is presented. In the next chapter the experimental set-up and characterization procedures will be described. This is followed by a detailed discussion on the results of the thin film sputtering, showing the impact of the deposition parameters on the thin film properties, loss figures and process stability.

Experimental set-up

For the Al_2O_3 layer deposition, an AJA ATC 1500 sputtering system has been applied. The schematic layout of this machine is depicted in Figure 1. The substrates, which can be up to 100-mm size, are introduced through a load-lock and are fixed on a substrate holder which can be rotated and heated up to a maximum temperature of 800 ^oC. The temperature of the heating element can be regulated within ± 3 ^oC. The background pressure of the deposition chamber can be pumped down to 2 x 10^{-7} mbar by a Turbo pump. The chamber pressure during deposition is adjusted by a valve to the pump and can be regulated within ± 0.1 mTorr. The system is equipped with three sputtering guns for 2-inch sputtering targets, which can be driven by either rf- or DC power supplies, both having a maximum range of 500 W. The power is typically set within ± 1 W. All sputtering guns are connected to an Ar line, which allows for a maximum Ar flow of 100 sccm controlled by flow controllers with an accuracy of 1%. The distance between the substrate holder and the sputtering target can be adjusted within a range of 10 to 18 cm. An oxygen flow controlled by a flow controller with 1% accuracy is connected to a gas inlet at the chamber. The oxygen allows for reactive co-sputtering of metallic targets. For the Al_2O_3 deposition, a high-purity 2-inch Al target is mounted to one of the sputtering guns. The general deposition procedure is as follows. After substrate loading the substrate rotation is switched on. Since preliminary tests have shown that this rotation speed has no impact on any of our layer parameters, it is fixed to a constant value for all processes. Then, the substrate is heated up to the deposition temperature followed by temperature stabilization for 15 minutes. After that the Ar and O_2 gas flows and the chamber pressure are adjusted to their process set-points. Then, the Al target is pre-sputtered at processing power and closed shutter for 5 to 10 minutes. The deposition starts by opening the shutter and after the deposition has been finished the procedure is followed in reverse order.

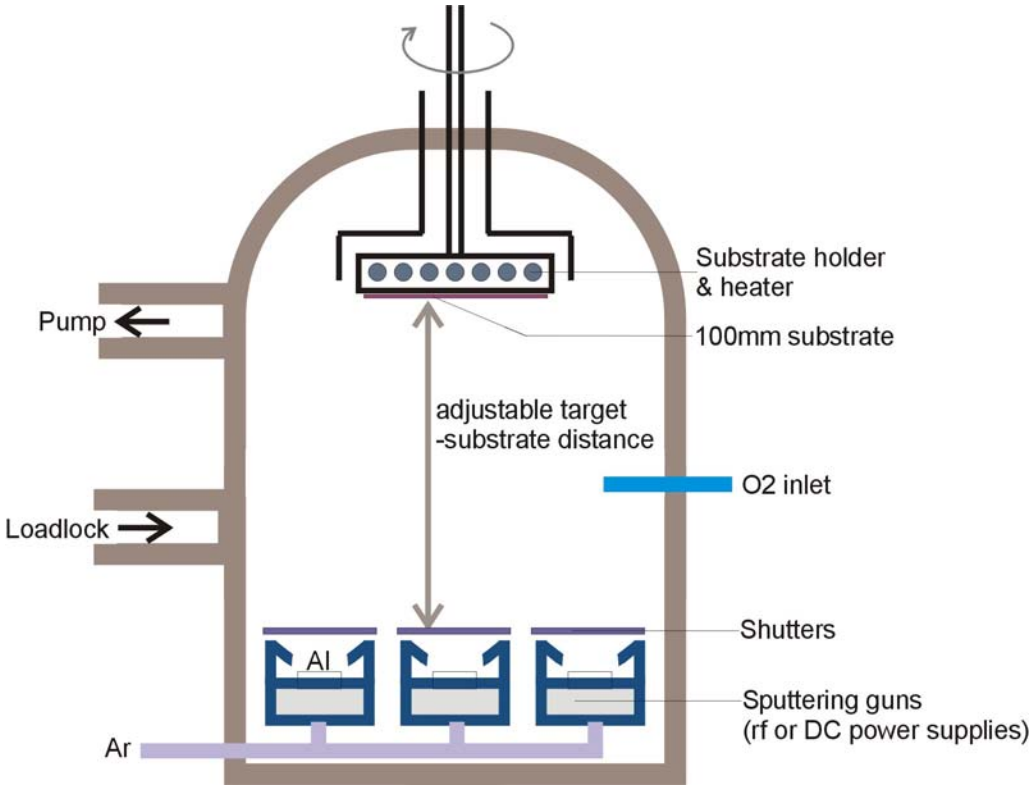

Figure 1: Schematic layout of deposition equipment for reactive co-sputtering

The deposition of Al_2O_3 films is carried out on 100-mm Si wafers, either bare or thermally oxidized to a thickness of 8 μm. The thin films grown on bare silicon are applied in ellipsometric inspection, whereas the layers grown on thermal oxide are suited for characterization by prism coupling. The thickness (d) and refractive index (n) of the layers are measured by a Woollam M44 ellipsometer and by a prism-coupling set-up (15). Moreover, the refractive index values for TE and TM polarized light have been determined by prism coupling. From those values, the material birefringence given by $\Delta n_{TM\text{-}TE} = n_{TM} - n_{TE}$ has been calculated. Both, prism coupling and ellipsometry (Plasmos SD 2000) have been applied for measuring the non-uniformity of the layer thickness (δd) and the refractive index (Δn) over the wafer. The non-uniformity has been determined over a 70 x 70-mm^2 area and will be defined as the half min-max value over the measured area. The optical loss of slab-type waveguides has been measured by the moving prism method (16).

For the determination of the layer density, the substrates have been weighted before and after the deposition on a 5-digit balance. Based on the weight difference and average layer thickness of the deposited film a straight-forward density calculation has been carried out. In order to calculate the stress of the thin films the wafer bow of the Si wafers has been measured over a length of 80 mm before and after the deposition. Combining data on the change in bow, layer thickness and substrate specific properties the stress value has been calculated.

Results & discussion

The impact of various processing parameters (temperature, pressure, power, total flow and oxygen percentage in flow) on the layer properties (deposition rate, refractive index, film density, stress, material birefringence and optical loss) has been studied for both, DC and rf-driven sputtering. The parameter range applied in this study is summarized in Table 1.

TABLE I. Summary of process parameters for preliminary study of Al_2O_3 layer properties upon deposition with DC and rf-based reactive co-sputtering.

Processing parameter	**DC based process**	**rf-based process**
temperature T [^{o}C]	400 - 500	400 - 500
pressure p [Pa]	1.5 – 3.5	2 – 4
Distance substrate-target [cm]	14 - 18	18
Power P [W]	150 – 275	150 - 250
total flow [sccm]	11 – 24.5	31.5 - 42
O_2 flow percentage [%]	10 - 25	5 – 10

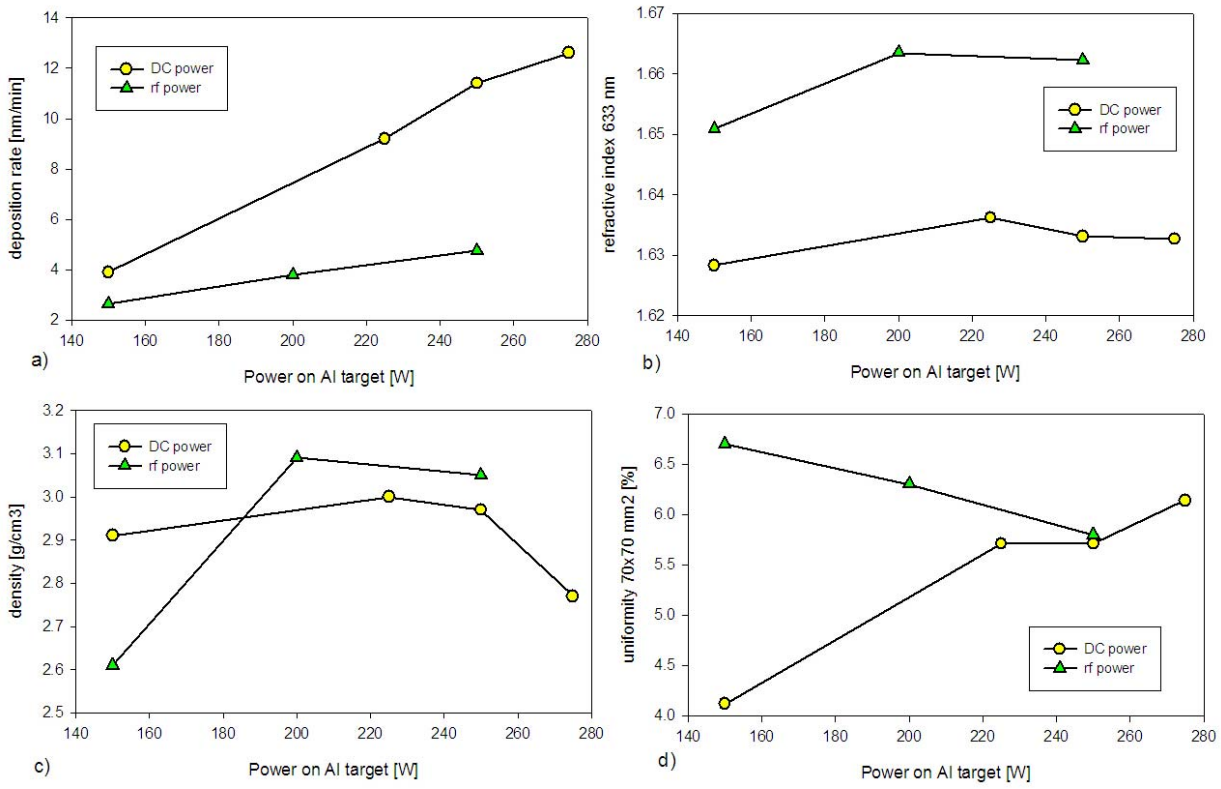

Figure 2: Impact of varied power on deposition rate (a), refractive index (b), density (c) and thickness uniformity (d) of deposited films of deposited films of Al_2O_3 films grown with DC and rf sputtering.

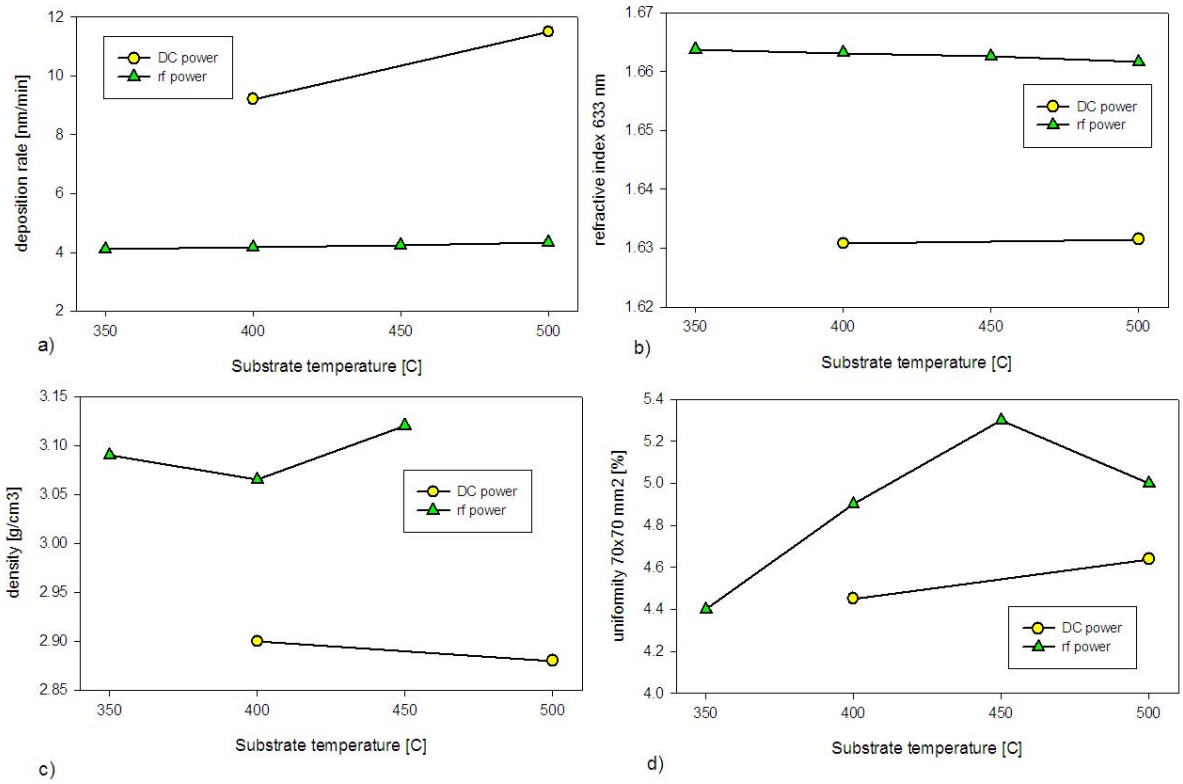

Figure 3: Impact of varied temperature on deposition rate (a), refractive index (b), density (c) and thickness uniformity (d) of deposited films of Al_2O_3 films grown with DC and rf sputtering.

Detail on the change of deposition rate, refractive index, density and thickness uniformity upon variation of power, temperature, pressure and total flow is shown in Figure 2, 3, 4 and 5, respectively. In general it can be seen that the deposition rate of the rf sputtered layers is a factor 2-3 lower than for DC grown layers, while the refractive index is clearly larger in case of the rf-based deposition. The deposition rate is mostly influenced by the sputtering power on the Al target, showing a nearly linear increase with the power. The refractive index changes most significantly as a function of chamber pressure; higher pressure results in a lower refractive index. The refractive index changes slightly upon variation in the lower power range and with the total flow and is almost unaffected by variation in the higher power range. In general a relation between the change in refractive index and the trends in the measured density can be observed, except for the dependence on the substrate temperature. Here we can notice a trend towards larger density at a (slightly) decreased refractive index. This observation can be explained by a higher surface mobility of the sputtered material at higher temperature resulting in fewer voids in the growing film in combination with a slightly lower refractive index due to a more complete oxidation of the Al bonds at elevated temperatures. Since both, voids in the film and incompletely oxidized Al bonds, will result in higher losses in the lower wavelength range, this is supported by the change in optical loss of waveguide deposited by rf sputtering and various temperatures (see Figure 6).

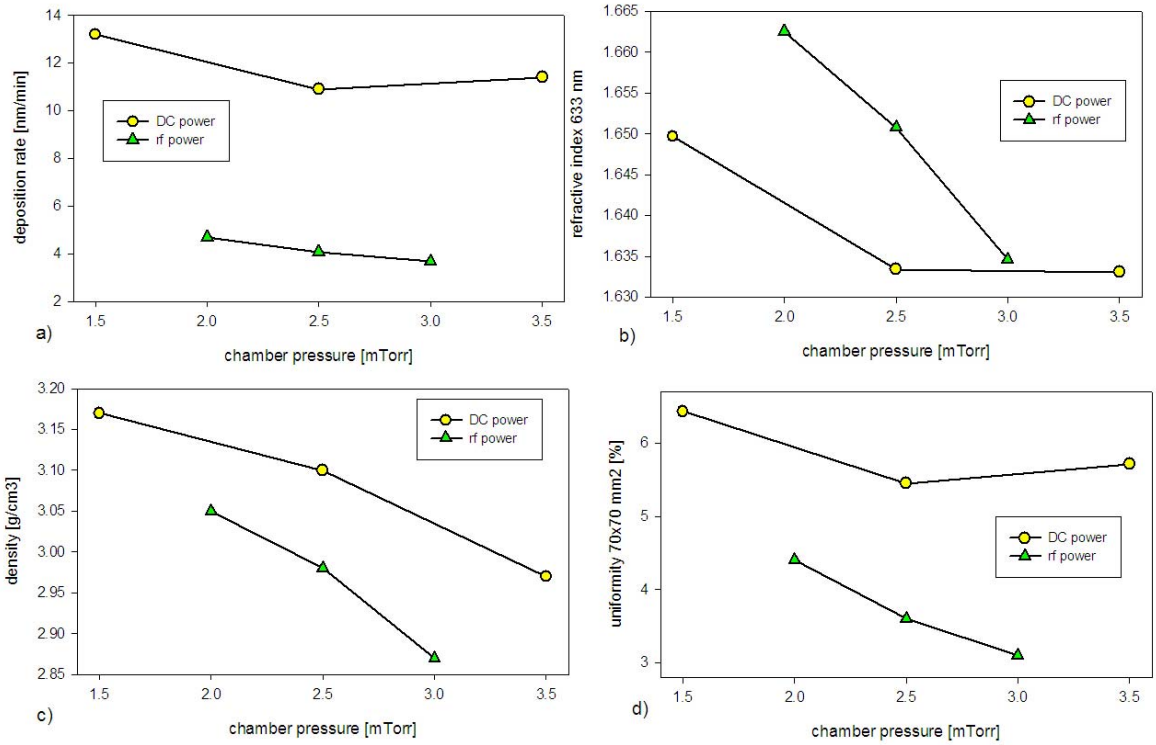

Figure 4: Impact of varied chamber pressure on deposition rate (a), refractive index (b), density (c) and thickness uniformity (d) of deposited films of Al_2O_3 films grown with DC and rf sputtering.

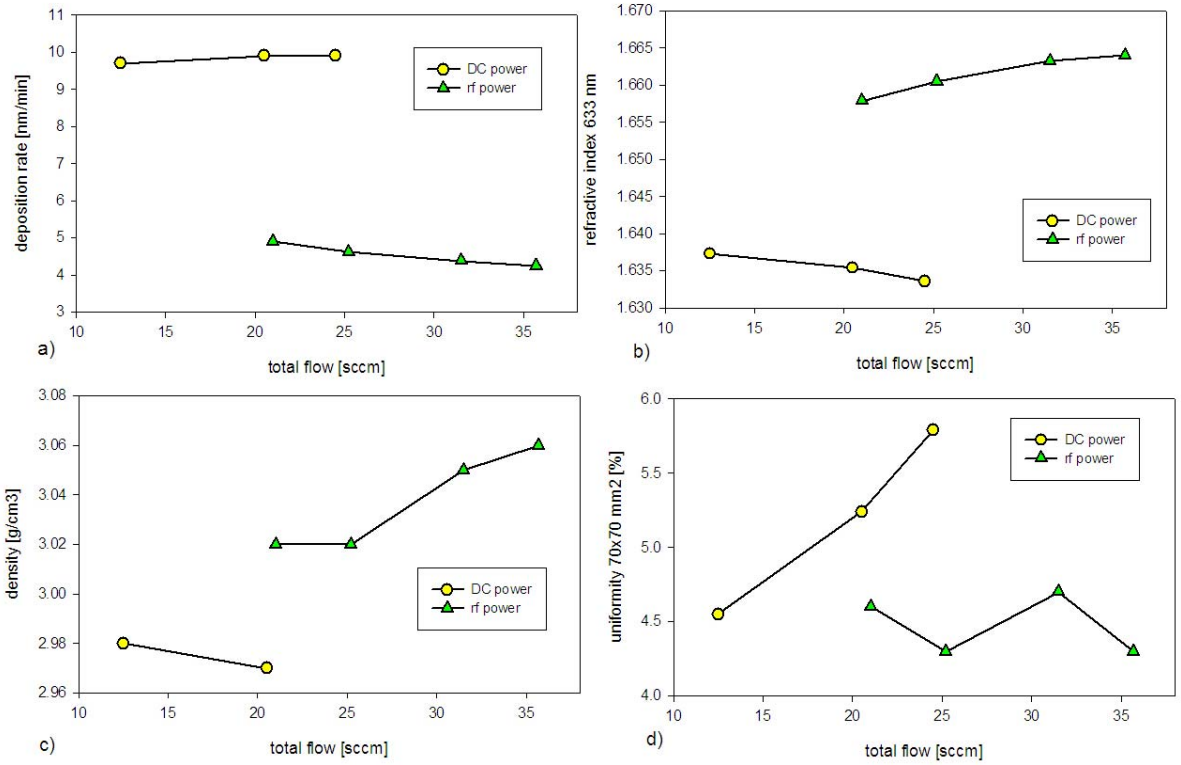

Figure 5: Impact of varied total flow on deposition rate (a), refractive index (b), density (c) and thickness uniformity (d) of deposited films of Al_2O_3 films grown with DC and rf sputtering. The DC and rf grown layers are deposited at constant oxygen flow and constant O_2 / Ar flow ratio, respectively.

Finally, the thickness uniformity is significantly influenced by all processing parameters. For low sputtering powers and high substrate temperatures the non-uniformity of the rf sputtered material is higher compared to the DC grown layers. In all other cases the uniformity of the rf-deposited films is either comparable or significantly better. Furthermore it should be noted that the non-uniformity over the 70x70 mm^2 area, which is typically in the range of 3-7 %, can be considered to be rather high, mainly when it is compared to values obtained in well-established Si-based integrated optics technology where uniformities are typically in the 1-2 % range. However, when taking into account the typical thickness distribution of the Al_2O_3 film over the wafer, which is depicted in the 9-point scan in Figure 7, it can be clearly seen that the non-uniformity rapidly increases towards the edge of the wafer. When taking into account a slightly smaller area (50x50 mm^2), the non-uniformity is decreased to ± 0.8%, what can compete well with the achievements in Si-based waveguide technology.

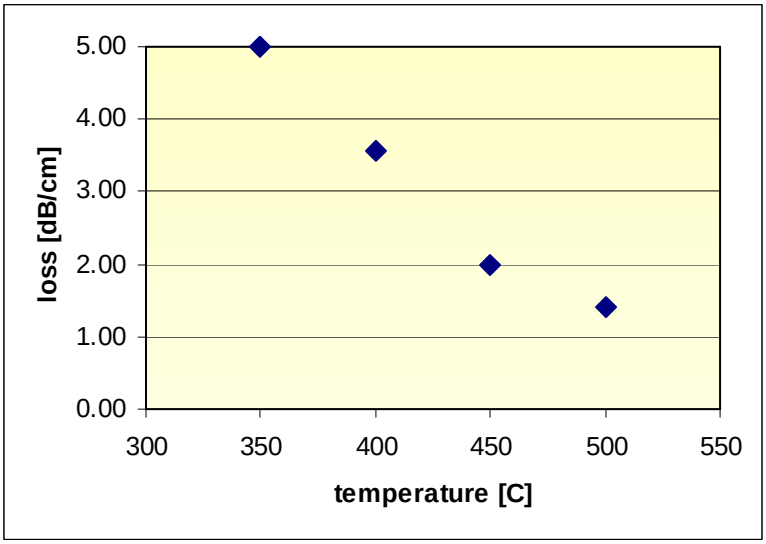

Figure 6: Change of optical loss of Al_2O_3 slab type waveguides at 633 nm wavelength as a function of deposition temperature.

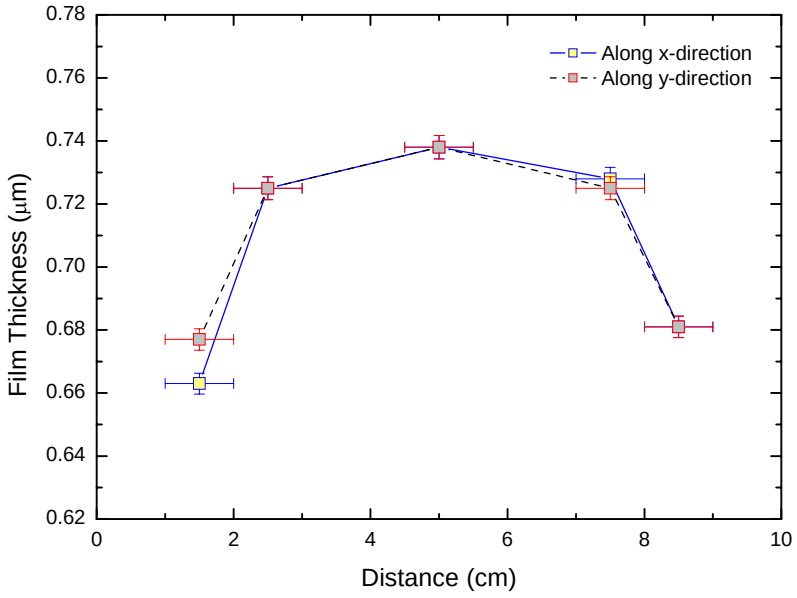

Figure 7: 9-point scan of layer thickness along two perpendicular directions on the 100-mm wafer.

The refractive index non-uniformity, measured by prism coupling, could be shown to be within the accuracy of the method, which is 5×10^{-4}.
The stress and birefringence in the thin films are generally low. For all layers, except for those grown at low temperature and low pressure, the stress is slightly tensile and varies within the range of 18-180 MPa. The stress decreases at higher power, temperature and pressure, while it inversely changes with the total flow. The material birefringence, defined as the difference of the refractive indices measured at TM and TE polarized light (n_{TM}-n_{TE}), is below the measurement accuracy of 10^{-3}. Since for many amorphous, dielectric thin films the material birefringence is attributed to the stress in the layer, the low birefringence in our Al_2O_3 waveguides is well in line with the low stress values.

Based on the above study on the rate, refractive index and uniformities of rf- and DC deposited films we can summarize that high substrate temperature, high sputtering power, low pressure and large total flow will result in optimized films with high refractive index and density and sufficiently large deposition rate for optical waveguide fabrication. From that point of view both methods, rf and DC sputtering, could be considered to be suited for integrated optical applications. The most striking difference between the two methods consists however in the process stability and the optical loss of the waveguides. In case of DC sputtering the optical quality is highly dependent on the exact condition of the sputtering target. Oxidation of the target surface can not be effectively removed by the DC power and upon a certain degree of oxidation large particles will be released from the target due to arcing. Pre-sputtering of the target prior to the deposition process delays the occurrence of arcing to some extend but is not an effective measure when relatively long deposition times are required in order to grow layers with typical waveguide thickness. In case of all waveguide samples fabricated by the DC sputtering process no propagation could be observed after coupling of light with a 633-nm wavelength. In contrary, the rf sputtering process was observed to be very stable and reproducible. The change of the deposition rate and the refractive index has been extracted from measurement of layer deposited under exactly the same processing conditions at various total thickness stages. As it can be seen in Figure 8b), the refractive index is reproduced within $\pm 10^{-3}$. The deposition rate, which is shown in Figure 8a), increases linearly as the target consumption progresses. This thickness change can be directly related to the decrease of the bias voltage on the sputtering target. Based on this direct relationship, the actual deposition rate can be calculated and a good control of the deposited thickness can be achieved by adjusting the deposition time accordingly.
Arcing has not been observed in the rf-sputtering process. In all optical waveguides light propagation could be shown upon coupling of 633 nm wavelength. Dependent on the exact processing conditions the optical loss at 633 nm wavelength varied between 1.4 and 8 dB/cm. The optical loss spectrum of a 660-nm thick Al_2O_3 waveguide deposited on 8-μm thermal oxide has been measured by the moving prism method. The optical loss throughout the near IR wavelength range of 1200-1600 nm is about 0.3 ± 0.15 dB/cm (see Figure 9). The relatively large measurement error is due to the fact that this loss range is around the limit of the applied method. Waveguide channel based loss characterization allowing for a significantly lower loss measurement limit is currently under investigation. Nevertheless, it should be noted that not only the loss performance is excellent, but also no loss increase around 1400 nm wavelength, which would be indicative for the presence of OH bonds, has been measured.

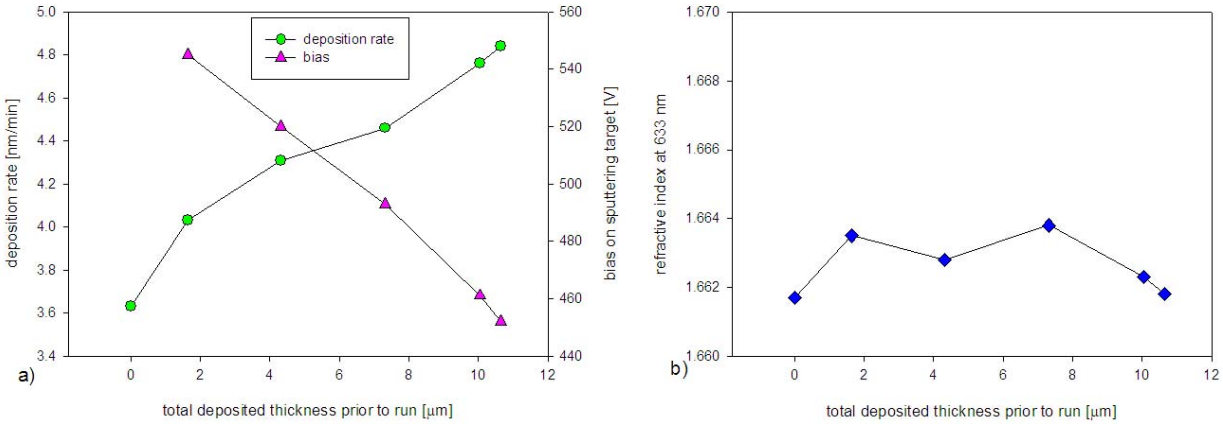

Figure 8: Reproducibility of deposition rate and refractive index as a function of the total layer thickness sputtered.

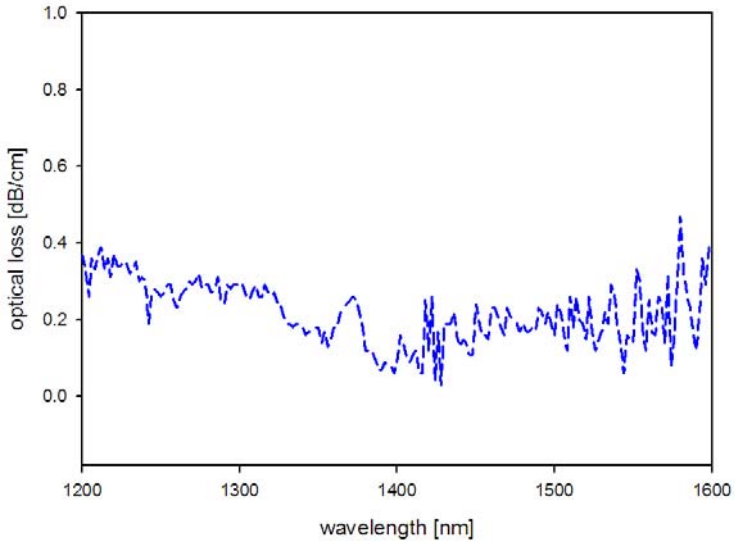

Figure 9: Optical loss spectrum at NIR wavelength of optimized Al_2O_3 layer deposited by rf-sputtering

Conclusions

It can be concluded that the Al_2O_3 layer deposition process has been successfully optimized. An rf-based reactive co-sputtering process, which resulted in stable, target condition-independent deposition of Al_2O_3 layers with high optical quality, has been developed. The optimized process enables uniform and reproducible waveguide deposition at a sufficiently high sputtering rate. The optical loss of waveguides based on the optimized material is 0.3 ± 0.15 dB/cm throughout the near IR wavelengths ranging from 1200 to 1600 nm. From this loss measurement it became evident that an OH absorption peak is absent. Therefore we expect that the optimized Al_2O_3 waveguide material will be well-suited for rare-earth-ion doped devices. Our future research will focus on channel waveguide light emitting structures employing this technology.

References

1. A. Suarez-Garcia, J. Gonzalo and C.N. Afonso, *Appl. Phys. A* **77**, 779-83 (2003).
2. A. Pillonnet, C. Garapon, C. Champeaux, C. Bovier, R. Brenier, H. Jaffrezic and J. Mugnier, *Appl. Phys. A* **69**, 735 (1999).
3. Y. Kim, S.M. Lee, C.S. Park, S.I. Lee and M.Y. Lee, *Appl. Phys. Lett.* **71**, 3604-3606 (1997).
4. S. Jakschik, U. Schroeder, T. Hecht, D. Krueger, G. Dollinger, A. Bergmaier, C. Luhmann and J.W. Bartha, *Appl. Surf. Science* **211**, 352-59 (2003).
5. M. Ishida, I. Katakabe, T. NN. Ohtake, *Appl. Phys. Lett.* **52**, 1326 (1988).
6. C.J. Kang, J.S. Chun and W.J. Lee, *Thin Solid Films* **189**, 161 (1990).
7. A. Pillonnet-Minardi, O. Marty, C. Bovier, C. Garapon and J. Mugnier, *Opt. Mat.* **16**, 9-13 (2001).
8. M. Benatsou, B. Capoen, M. Bouazaoui, W. Tchana and J.P. Vilcot, *Appl. Phys. Lett.* **71**, 428 (1997).
9. X.J. Wang and M.K. Lei, *Thin Solid Films* **476**, 41-45 (2005).
10. M.K. Smit, G.A. Acket and C.J. van der Laan, *Electronics and Optics* **138**, 171-81 (1986).
11. S.M. Arnold and B.E. Cole, *Electronics and Optics* **165**, 1-9 (1988).
12. B.J.H. Stadler, M. Oliviera and L.O. Bouthillette, *J. Am. Ceram. Soc.* **78**, 3336-44 (1995).
13. S. Musa, H.J. van Weerden, T.H. Yau and P.V. Lambeck, *IEEE J. Quant. Electr.* **36**, 1089-97 (2000).
14. G.N. van den Hoven, J.A. van der Elsken, A. Polman, C. van Dam, K.W.M. van Uffelen and M.K. Smit, *Appl. Opt.* **36**, 3338-41 (1997).
15. K. Wörhoff, P.V. Lambeck, H. Albers, O.F.J. Noordman, N.F. van Hulst and Th.J.A. Popma, in *Micro-optical technologies for measurement, sensors and microsystems II and optical fiber sensor technologies and applications,* O. Parriaux, E.B. Kley, B. Culshaw and M. Breidne, eds., Proc. of SPIE **3099**, 257 (1996).
16. T.H. Hoekstra, *Ph.D. thesis*, University of Twente, Enschede (1994).